Universiteit Leiden
The Netherlands

Towards a single-molecule FRET study of Frauenfelder's nonexponential rebinding of CO in myoglobin

Eskandari Alughare, Z.

Citation
Eskandari Alughare, Z. (2022, June 23). *Towards a single-molecule FRET study of Frauenfelder's nonexponential rebinding of CO in myoglobin*. *Casimir PhD Series*. Retrieved from https://hdl.handle.net/1887/3348505

Version:	Publisher's Version
License:	Licence agreement concerning inclusion of doctoral thesis in the Institutional Repository of the University of Leiden
Downloaded from:	https://hdl.handle.net/1887/3348505

Note: To cite this publication please use the final published version (if applicable).

1
Introduction

Optical single-molecule techniques emerged more than 30 years ago with experiments monitoring single probe molecule behavior in solids at cryogenic temperatures and extended to much higher temperatures. Single-molecule microscopy enable the imaging of biological structures such as proteins at resolutions close to the molecular scale to determine the individual molecules' behaviors and elucidation of the distribution, rather than the average.

Early time-resolved experiments by Frauenfelder on the ensemble of the kinetic rebinding of CO to myoglobin molecules resulted in a stretched exponential relaxation due to a very large spread of the reaction rates of individual molecules. These results were assigned to the heterogeneity in this system originated from different conformations of different single-molecule proteins and from the widely different reaction rates associated with each of these conformations. This approach marked the beginning of a new area in the physical chemistry of proteins. The research to image this heterogeneity in this system with single molecule microscopy is still missing.

The work presented in this thesis contains two lines of research. On the one hand, we investigate the Förster Resonance Energy Transfer (FRET) of dye labeled-carboxymyoglobin (MbCO) in the ensemble to show the feasibility of performing single molecule-FRET experiments to study the kinetic rebinding of CO to myoglobin. On the other hand, we study the Förster theory about a stretched-exponential fluorescence intensity decay under ensemble conditions for a distribution of acceptors in the vicinity of each donor; This non-exponential kinetics arise from a distribution of the exponential steps originated from different single molecules. Using single-molecule microscopy, we study the histograms of the decay rates of single fluorophore molecules (donor) in the presence of acceptors as exponential which average out as non-exponential decay in the ensemble.

In this introduction chapter, we briefly describe the experimental techniques we used and the main characteristics of the systems we worked with. More detailed discussions will be given in the respective chapters.

1.1 Luminescence

Luminescence is any process where photons are spontaneously emitted not because of heat, in the visible, ultraviolet, or infrared spectral range. [1,2] Based on the process leading to the emission of the electromagnetic radiation, there are different kinds of luminescence such as photoluminescence, [3,4] chemiluminescence, and electroluminescence. [5]
Photoluminescence is one form of luminescence in which a material is first excited by electromagnetic radiation, which causes an electron from the ground state to go to a higher energy level in an atom or molecule. The excitation is followed by re-radiation. [6] Photoluminescence spectroscopy is widely used to characterize the optical and electronic properties of photoluminescent molecules and mostly is referred to as fluorescence spectroscopy. [7] As very few biomolecules are naturally fluorescent, they are generally labeled with fluorescent dyes to make them detectable.

1.2 Fluorescence spectroscopy

Photoluminescence can refer to either a fluorescence or a phosphorescence process. Fluorescence excitation and detection is the most common and important method in light microscopy, thanks to its high sensitivity and specificity. In fluorescence, the emitting species first absorbs an excitation photon, which brings it from its ground electronic state (usually a singlet spin state) to one of the vibrational states of an excited electronic state (usually another singlet state). The excited molecule loses excess vibrational energy through interactions with the surrounding medium, and relaxes to the lowest vibrational state of its excited electronic state. Thereafter, the excited molecule, without changing its spin, emits a photon with a longer wavelength than the excitation photon. The electronic transitions of molecules are often illustrated in an energy level diagram called the Jablonski diagram (Figure 1.1). The diagram shows the absorption process consisting of the excitation of an electron from the singlet ground state (S_0) to one of the vibronic levels of the singlet excited state (S_1). Then the molecule relaxes non-radiatively to the first vibrational level of the singlet excited state through the dissipation of energy towards other molecules in the environment. [8,9]
In phosphorescence, similar to fluorescence, the species after photon excitation emits a photon to the ground state with a longer wavelength than the excitation radiation. However, this relaxation is accompanied by a change in the electron spin in which the excited molecule goes through intersystem crossing from a singlet state (S_1, or S_2) to a state with a different spin multiplicity, usually a triplet state (T). This results in a longer lifetime of the excited state (milli seconds to minutes, see Figure 1.1). [8–10]
Some nonradiative transitions are known to occur through different mechanisms such as internal conversion (IC), intersystem crossing (ISC) (Figure 1.1), and collisional quenching. Non-radiative IC is a process in which a photoexcited molecule in a vibrational excited state relaxes to a vibrational state of a lower electronic state in a time of the order of a few ps. [8,11] ISC is a transition of a photoexcited molecule from its singlet excited state to a state with a different spin multiplicity (triplet state) usually on the μs time scale. [8,12] Collisional quenching is another deactivating process in which the excited state of the fluorophore loses energy by energy transfer to a quencher or by other relaxation processes induced by interactions with the surrounding molecules in the solution. In the case of quenching by species *Q*, the

fluorescence intensity of the fluorophore decreases according to the Stern–Volmer equation": [8,13,14]

$$\frac{I}{I_q} = 1 + K_{SV}[Q] = 1 + k_q \tau [Q] \qquad 1.1$$

where I is and I_q are the fluorescence intensity of fluorophore in the absence and presence of the quencher, K_{SV} presents the Stern–Volmer quenching constant, and k_q, τ, and $[Q]$ are the bimolecular quenching constant, the lifetime of fluorophore in the absence of quencher, and the concentration of quencher, respectively.

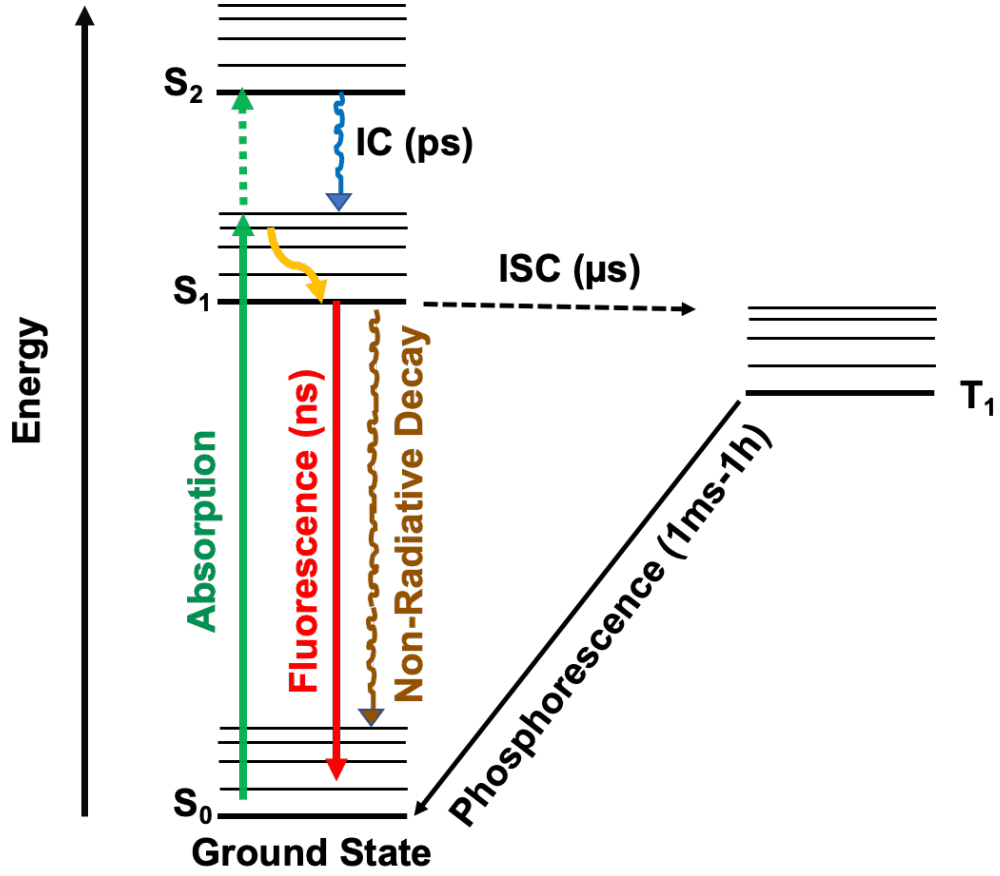

Figure 1.1 *A Jablonski diagram illustrating the following processes: light absorption including an electronic transition $S_0 \rightarrow S_1$ (green arrow), a non-radiative transition (orange arrow), fluorescence $S_1 \rightarrow S_0$ (red arrow), non-radiative decay (brown arrow), IC (blue arrow), ISC (dashed black arrow), and phosphorescence $T_1 \rightarrow S_0$ (black arrow). The states involved are the singlet ground state (S_0), singlet excited states (S_1, S_2) and the triplet excited state (T_1) [modified after [8]].*

Fluorescence is widely used in different areas particularly in cellular biochemistry and biomedicine. Fluorescence-based assays are widely used, specially in the biomedical science and allow one to discover the details of the molecular mechanisms in biological reactions. Fluorescent experiments can be performed in real-time in

ensembles and at the single- molecule level and constitute a practical tool for measuring biomolecular conformational changes, probing protein–nucleic acid interactions, etc. [15–17]

1.3 Properties of fluorophores

1.3.1 Molar absorption coefficient

A well-known intrinsic property of a chemical species is its molar extinction coefficient (ε) which indicates how strongly a chemical species or substance absorbs the light at a determined wavelength. Thus, the higher extinction coefficient, the greater the amount of light being absorbed. ε is constant for a specific compound at a certain wavelength under fixed conditions, for example solvent, pH and temperature. Since it is a substance-specific constant under those conditions, chemists frequently use ε to measure the concentration of chemicals, e.g., proteins in solution.
The absorption process can be described by the Beer-Lambert Law: [18]

$$A = \varepsilon bc \qquad 1.2$$

where *A* is the absorbance, ε is the molar extinction coefficient, b is the optical path length through the solution and *c* is the concentration of the species.
The brightness of a fluorescent molecule can be calculated from the molar extinction coefficient at the excitation wavelength and the fluorescence quantum yield as efficiency of fluorescent emission by using the following equation: [19]

$$\text{Brightness} = \varepsilon\phi \qquad 1.3$$

where ϕ is the quantum yield discussed below.
Basically, the brightness depends on how strongly a fluorophore absorbs the light (ε) and how well it emits the light (ϕ). Fluorophores with a high quantum yield and extinction coefficient are the brightest.

1.3.2 Quantum yield

Not all of the light absorbed by a fluorophore is completely re-emitted as light during relaxation to the ground state, because some non-radiative decay processes compete with photon emission as described in section 1.2. The fluorescence quantum yield (ϕ) is defined as the number of photons emitted by the excited fluorophore divided by the number of absorbed photons. ϕ is calculated from the ratio of the radiative decay rate (k_r) to the total fluorescence decay rate (k_f), including radiative and non-radiative channels: [20]

$$\phi = \frac{k_r}{k_r + k_{nr}} \qquad 1.4$$

According to the above equation, when the radiative rate (k_r) is high and the non-radiative rate (k_{nr}) is low, ϕ will be large, whereas a non-fluorescent fluorophore has a quantum yield of zero.
The magnitude of k_{nr} depends strongly on the local environment whereas k_r is essentially determined by the electronic structure of fluorophore.

1.3.3 Fluorescence lifetime

When a fluorophore is photoexcited, it relaxes to the ground state through radiative and/or nonradiative pathways. The relation between the fluorescence decay rate and the fluorescence decay time is described according to: [21]

$$I_t = I_0 e^{-t/\tau} \quad 1.5$$

$$\frac{1}{\tau} = \sum k_i \quad 1.6$$

where t is the time, τ the fluorescence lifetime, I_0 and I_t the fluorescence intensity at time zero (t = 0), and at time t, respectively. k_i are the decay rates for the various decay pathways, for example the radiative decay rate, k_r, or the non-radiative decay rate, k_{nr}.
These radiative and non-radiative rates determine the quantum yield, fluorescence intensity, and lifetime. The lifetime is characteristic of the electronic properties of the fluorophore but is influenced by the surrounding environment. Lifetime is the parameter that is most easily measured precisely and is least affected by the equipment.

1.4 Fluorescence resonance energy transfer (FRET)

FRET, first described by Theodor Förster, [22] is a process by which the excitation energy is transferred nonradiatively from a photoexcited donor fluorophore to an acceptor fluorophore over distances of 10-90 Å (Figure 1.2). Thus, when a chromophore is photoexcited to an excited state, instead of directly relaxing to the ground state by fluorescing, it may transfer its energy to the excited state of an acceptor chromophore in the vicinity (10-90 Å) through nonradiative dipole–dipole coupling. The efficiency of the FRET process scales with the inverse sixth power of the distance between the donor and acceptor. Thus, this technique is highly sensitive to changes in distance on the scale of Angstroms. Since energy transfer occurs through dipole–dipole coupling, the FRET efficiency also depends on the orientations of donor and acceptor dipole moments with respect to each other and to the radius vector between their centers. [23]

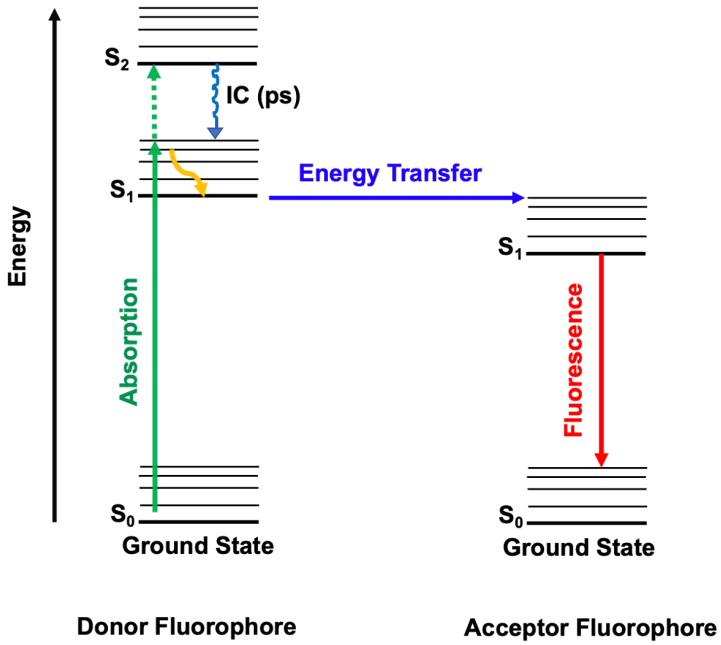

***Figure 1.2**. A Jablonski diagram illustration for FRET. The singlet ground and excited states S_0, S_1, and S_2 of the donor are shown on the left side with excitation and de-excitation pathways. On the right side of the figure, the ground state S_0 and first excited state S_1 of an acceptor for FRET are shown together with the energy transfer pathway from the donor S_1 state to the acceptor S_1 state [after [8]].*

The FRET efficiency *E* is defined as the fraction of donor excitations that result in energy transfer and it is determined by the ratio of the energy transfer rate k_{ET} to the sum of all rates depopulating the excited state of the donor: [23]

$$E = \frac{k_{ET}}{k_{ET} + k_r + \sum k_i} \qquad 1.7$$

where k_{ET} is the rate of energy transfer, k_r, the radiative decay rate of the donor, k_i the rates of any other nonradiative de-excitation pathways not involving FRET.

The Förster radius R_0, i.e. the distance at which the energy transfer efficiency is 50%, depends on the overlap of the donor emission spectrum with the acceptor absorption spectrum and on their mutual molecular orientation as expressed by the following equation: [24]

$$R_0 = 0.2108\left(\frac{\phi_D \kappa^2}{n^4} \int \bar{F}_D(\lambda)\epsilon_A(\lambda)\,\lambda^4 d\lambda\right)^{\frac{1}{6}} \qquad 1.8$$

where ϕ_D is the fluorescence quantum yield of the donor in the absence of the acceptor, κ^2 is the dipole orientation factor which can change between 0 and 4, n is the refractive index of the medium, $\epsilon_A(\lambda)$ is the acceptor molar extinction coefficient ($M^{-1}cm^{-1}$), and $\bar{F}_D$ is the donor emission spectrum normalized to an area of 1 ($\int_0^\infty F_D\,(\lambda)d\lambda = 1$).

As the FRET efficiency is inversely proportional to the sixth power of the distance between donor and acceptor chromophores, it is possible to measure small changes in this distance. FRET has emerged as a powerful fluorescent spectroscopic technique in cell biochemistry and biophysics to measure structural dynamics, kinetics, and for mapping the conformations of biomolecules in complex systems.

1.4.1 Distance between donor and acceptor

As mentioned before, the energy transfer efficiency (*E*) depends inversely on the 6th-power of the distance between the donor and acceptor (*r*), due to the dipole–dipole coupling mechanism (Figure 1.3 A): [24]

$$E = \frac{1}{1+\left(\frac{r}{R_0}\right)^6} \qquad 1.10$$

According to this equation, any event or process that alters the distance between donor and acceptor will strongly change the energy transfer rate and allow one to observe biomolecular conformational changes in a time range of ps-ms on a nanometer scale by measuring the resonance energy transfer.
Based on the Eq. 1.8, due to the λ^4 dependence of the overlap integral, small shifts in the spectra can have large effects on the R_0. The following sections describe two factors: the overlap integral and the orientation factor (κ^2), that influence R_0 and the FRET efficiency.

1.4.2 The overlap integral

The rate of energy transfer depends on how well the donor emission spectra and acceptor absorption spectra overlap (Figure 1.3B). [24]

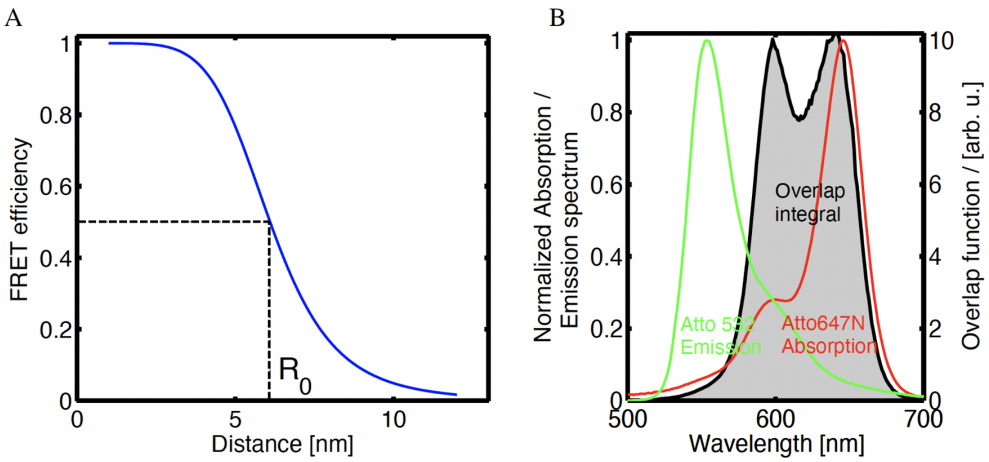

Figure 1.3 (A) *Dependence of the FRET efficiency on the distance between the donor (Atto 532) and acceptor fluorophores (Atto 647N). For this donor-acceptor pair, the calculated Förster radius is R_0 = 6.1 nm, at which distance the FRET efficiency (E) is 50%.* ***(B)*** *The grey colour area is a visualization of the overlap between the emission spectrum of donor (Atto 532, green colour) and acceptor emission spectra (Atto 647N, red colour). The overlap integral is proportional to the area under this curve (gray area), based on equation 1.8 (as* $\int \bar{F}_D(\lambda)\epsilon_A(\lambda)\,\lambda^4 d\lambda$*).* [25]

The phenomenon of fluorescence resonance energy transfer does not require the acceptor to be fluorescent. In this case, after excitation of the donor the donor fluorescence is quenched by the acceptor and the fluorescence intensity and lifetime of the donor will change. (Figure 1.4B).

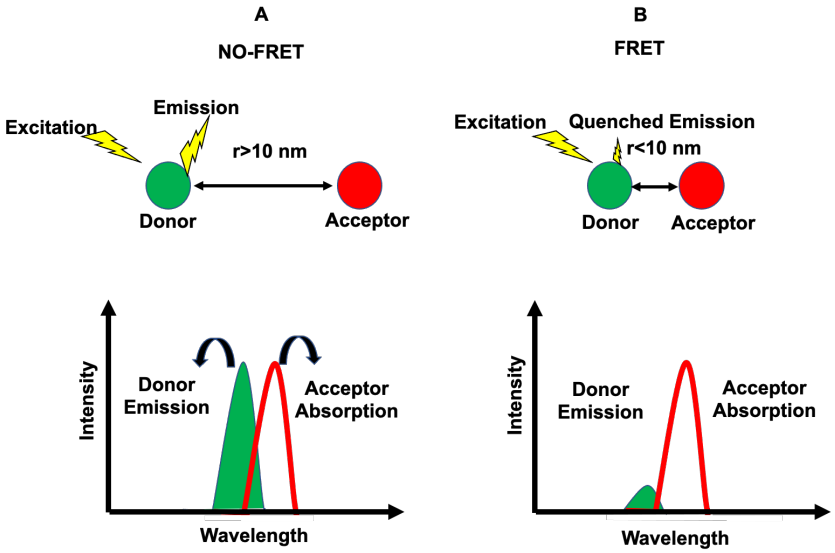

Figure 1.4 *Schematic of FRET in the presence of a non-fluorescent quenching acceptor (A) describes No FRET because of r>10 nm, (B) FRET occurs (r<10 nm) after excitation of donor. The fluorescence emission of the donor is quenched by the acceptor. The acceptor does not fluoresce but the intensity and lifetime of the donor change.* The donor and acceptor shown in green and red colours respectively.

In most applications, however, both donor and acceptor are fluorescent, and in most cases, the energy transfer occurs through quenching of the donor fluorescence and a reduction of the donor fluorescence lifetime, and an increase in the intensity of the acceptor fluorescence (Figure 1.5B).

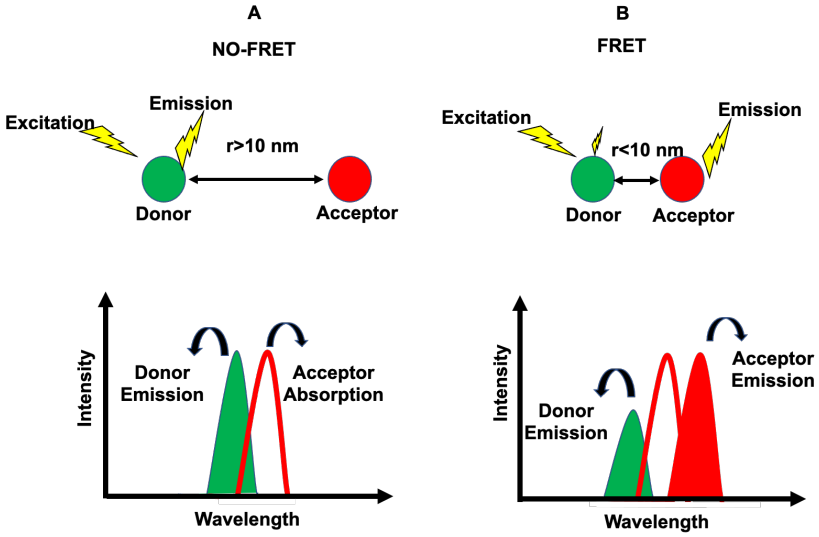

Figure 1.5 *Schematic of FRET in the presence of a fluorescent quenching acceptor (A) describes No FRET because of r>10 nm, (B) FRET occurs (r<10 nm) after excitation of donor. The energy is transferred from donor to the acceptor. In this case,* both donor and acceptor are fluorescent. Donor and acceptor have been shown in green and red colours respectively.

1.4.3 The orientation factor κ^2

Since energy transfer occurs through dipole–dipole coupling, the FRET efficiency also depends on the orientations of donor and acceptor dipole moments with respect to each other and to the radius vector between their centers.

The orientation factor (κ^2) depends on how the donor emission dipole and the acceptor absorption dipole are oriented relative to each other. κ^2 can range from zero to 4, however, it is typically assumed to be the dynamically averaged value of 2/3 (0.67) (Figures 1.6A).

When the donor emission dipole and the acceptor absorption dipole are parallel and they are perpendicular to the donor-acceptor radius vector, the value of κ^2 is 1 (Figure 1.6B), whereas for perpendicular transition moments of donor and acceptor in the same spatial disposition, κ^2 is zero (Figures 1.6 C). The κ^2 factor has a maximum value of 4 when the dipoles are parallel and lie along the radius vector. [26]

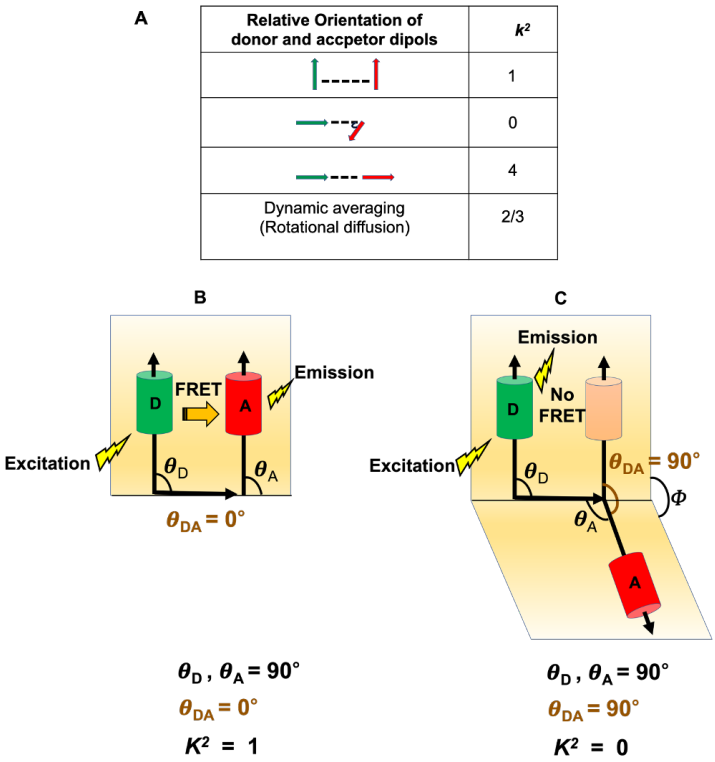

Figure 1.6 *The orientation factor κ^2 (A) The various orientations of the donor-acceptor dipoles. (B) example where the donor emission dipole and the acceptor absorption dipole are parallel, and (C) where the donor emission dipole and the acceptor absorption dipole are perpendicular relative to the molecular connection radius vector. The donor (green) emission dipole D and the acceptor (red) absorption dipole A, and the vector connecting the donor emission and acceptor absorption dipoles are shown by the black arrows. The angles θ_D and θ_A are the angles between the line connecting the dipoles and the dipoles D and A, respectively. θ_{DA} is the angle between the emission transition dipole of the donor (purple) and the absorption transition dipole of the acceptor (when the distance is zero), and ϕ is the angle between the planes containing the two transition dipoles (planes shown in yellow) [after [27]].*

The dependence of the orientation factor (κ-squared) on the relative orientations of the donor emission dipole and the acceptor absorption dipole (illustrated in Figure1.6A) is given by the equation: [27,28]

$$\kappa^2 = (\cos\theta_{DA} - 3\cos\theta_D \cos\theta_A)^2 = (\sin\theta_D \sin\theta_A \cos\Phi - 2\cos\theta_D \cos\theta_A)^2 \quad 1.11$$

where θ_{DA} is the angle between the emission transition dipole of the donor and the absorption transition dipole of the acceptor, θ_D and θ_A are the angles between these dipoles and the radius vector joining the donor and acceptor, and Φ is the angle between the planes containing the two transition dipoles.

1.5 Ensemble and single-molecule spectroscopy

Ensemble fluorescent assays from a homogeneous sample provide a value for the experimental observables that depend on the molecular properties of the sample. However, fluorescence spectroscopy of a non- homogeneous ensemble sample that consists of several different subpopulations similarly reports an average value of the molecular parameters, which depends on the nature of the heterogeneity. In a non-homogeneous ensemble sample, each molecule has a different environment, and interaction. Thus each individual molecule behaves differently and ensemble fluorescence assays only report the mean value of the fluorescent measurement and do not give any information about individual molecules. [27,29]

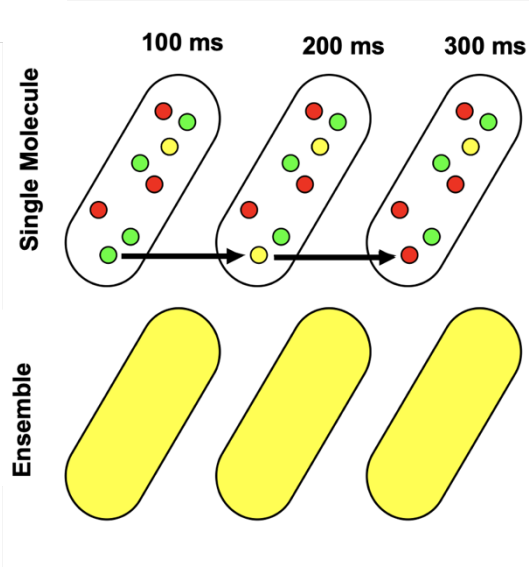

Figure 1.7 *A scheme illustrating the difference between single-molecule (top) and ensemble detection (bottom) for the static and dynamic heterogeneities in a sample. In this illustration, a biomolecule has, for instance, three different states depicted in the three colors: red, yellow, and green (static heterogeneity) and biomolecules can interconvert between these three states every 100-ms (dynamic heterogeneity). Single-molecule techniques can detect and distinguish both static heterogeneity and dynamic heterogeneity, whereas ensemble techniques only measure average values* . [28]

A fundamental advantage of smFRET (single-molecule FRET) is its ability to resolve sample heterogeneity and to provide distributions of quantities related to the different subpopulations in the sample. For example, in an ensemble, it is impossible to detect the dynamic switching of a protein between different states over the course of the experiment, but it can be measured by smFRET. Single-molecule spectroscopy has several known advantages: a high sensitivity to nano-meter distances (1-10 nm), the ability to measure a single molecule, the ability to measure structural and dynamic heterogeneities, and a high sensitivity and specificity to the labelled molecules, because only the fluorescence signal of label molecules is detected, even in a crowded environment. [24]

1.6 Confocal microscopy

Although the number of single-molecule methods is continuously increasing and each of them has specific advantages and disadvantages, detection of single molecules with a confocal microscope makes the observation of individual molecules possible with a simple setup. [30] Confocal microscopy was invented by Marvin Minsky in the late 1950s. [31] His confocal setup was made of a lamp, a pinhole, a lens, and a detector. The principle of a confocal microscope is to produce a point source of light in a focal plane and reject all photons from the out-of-focus planes to increase the optical resolution and the image contrast. Figure 1.8 demonstrates a general confocal setup in which the excitation photons from a laser are sent to a single spot in the sample through an objective. The fluorescence photons emitted by the sample are transmitted by a dichroic mirror, focused by suitable lenses, pass through a pinhole positioned so that only photons from the objective's focus pass whereas photons emitted by out-of-focus planes are mostly rejected. Photons from the in-focus excitation point finally reach the detector after spectral filtering by a long-pass fluorescence filter. By raster-scanning the focal plane, one obtains a fluorescence image. Technological advances have increased the sensitivity and lowered the pixel dwell times in confocal microscopy, making it today an ideal tool for fluorescence microscopy. [32]

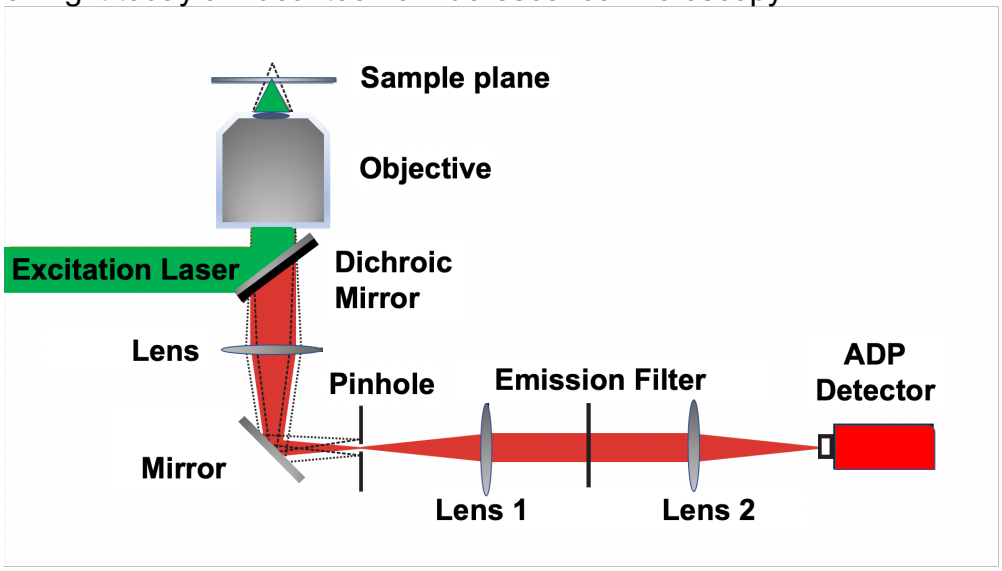

Figure 1.8 *Schematic of a general confocal setup. The laser sends excitation photons (green) into the objective by a dichroic mirror. Fluorescence light (red) emitted from the plane of sample arrive at a pinhole and only the photons emitted from the focus of the objective pass through and reach the detector, an avalanche photodiode (APD) in this case [modified after [25]].*

1.6.1 Time-Correlated Single-Photon Counting (TCSPC)

It is essential for fluorescence lifetime measurements to determine the exact arrival time of individual fluorescence photons. TCSPC is a tool to precisely record the arrival time of each photon upon excitation by a laser pulse. The laser has a high repetition rate (around 80 MHz) and delivers short pulsed (ps) pulses. APDs produce one electrical pulse for each detected photon. The fluorescence decay profile is obtained based on the detection at a multitude of single photon events, which are collected over many cycles. The synchronization is controlled by the laser driver "Sepia I". [33]

1.7 Proteins

Proteins are known as essential molecular machines in the cells which are responsible for many vital functions. Such proteins as enzymes, hormone receptors, regulatory and transport proteins, are indispensable key molecules in such vital processes as immunity, circulation, and homeostasy. In 1838, Gerardus Mulder was the first who introduced the word protein in his publication and he defined it as: " The *name protein that I propose for the organic oxide of fibrin and albumin, I wanted to derive from Greek word proteios, because it appears to be the primitive or principal substance of animal nutrition*". [34]
Proteins are complex polymers made of monomeric amino-acid units linked together. A protein chain is a sequence of amino-acids taken out of 20 different compounds, and arranged in a specific order. Which amino-acid comes next upon protein synthesis is determined by a codon of three nucleotides in the DNA or RNA of the cell coding for that protein. The number of amino acids in a protein varies from 50 to more than 30,000 amino-acids. Macromolecules which have less than 50 amino acids are called peptides.
The structure of a protein determines its function in the living organism. Importantly, the conditions in the surroundings of a protein, such as pH, temperature, and salt concentration, have a direct effect on the protein structure and consequently on the protein function. One distinguishes four levels in the structure of proteins: primary structure, secondary structure, tertiary structure and quaternary structure. [34]

1.7.1 Primary Structure

The chemistry of amino acid side chains is important in the formation of protein structure. In general, an amino acid consists of an alpha carbon (Cα) bound to three different substituents comprising an amine (via a nitrogen atom), a carboxylic carbon (via a carbon atom), and a hydrogen (Figure 1.9). [35]

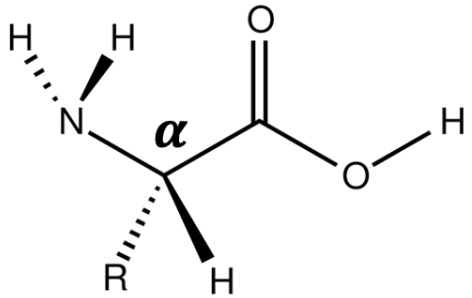

Figure 1.9 *Chemical structure of an amino-acid.* [35]

The reaction between two amino-acids in which the carboxylic group of an upstream amino-acid (Figure 1.9A left) and the amine group of a downstream amino-acid (Figure 1.10 A, right) condense by losing a water molecule, results in the formation of a peptide bond (Figure 1.10B). Polypeptides are formed by successive dehydration reactions between successive amino-acids (Figure 1.10C). The primary structure is constituted by this specific sequence of amino-acids bound by peptide bonds into a polypeptide chain (Figure 1.10 D).

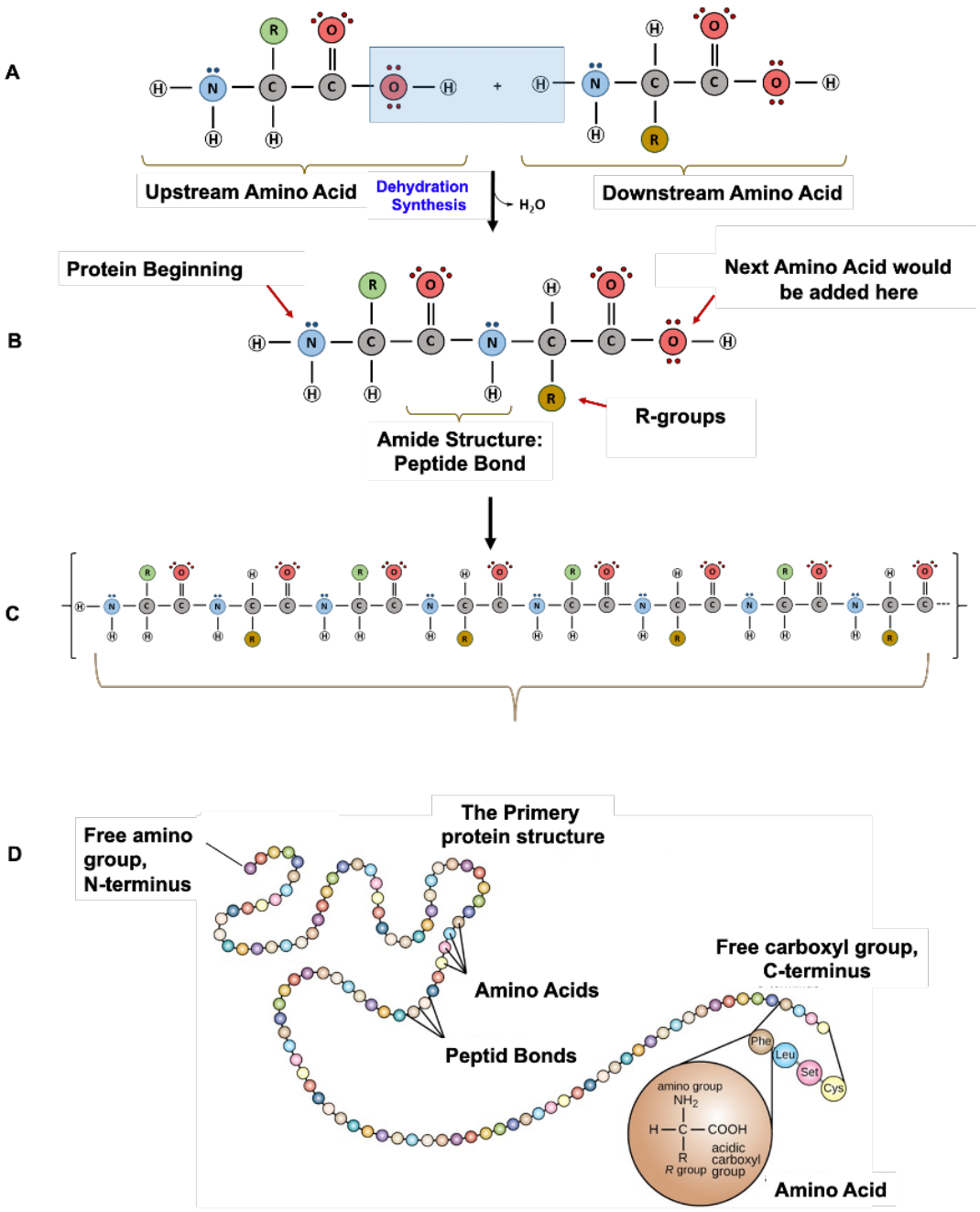

Figure 1.10 Formation of the primary protein structure (A-D). *The dehydration reaction between two amino-acids form a peptide bond and successive dehydration steps produce a polypeptide with the primary protein structure [modified after* [36]*]*

1.7.2 Secondary Structure

The first folding step of a protein chain gives rise to the secondary structure, stabilized by hydrogen bonds between the C=O and H-N groups. The secondary structure depends on the amino-acid sequence and often belongs to one of two main folding forms: alpha-helix or beta-sheet (Figure 1.11). An alpha-helix can have either of two conformations, right-handed or left-handed. The beta-sheet has two anti-parallel and parallel conformers. These two folding forms produce a hydrophobic core and a hydrophilic surface in a protein [37] (Figure 1.11).

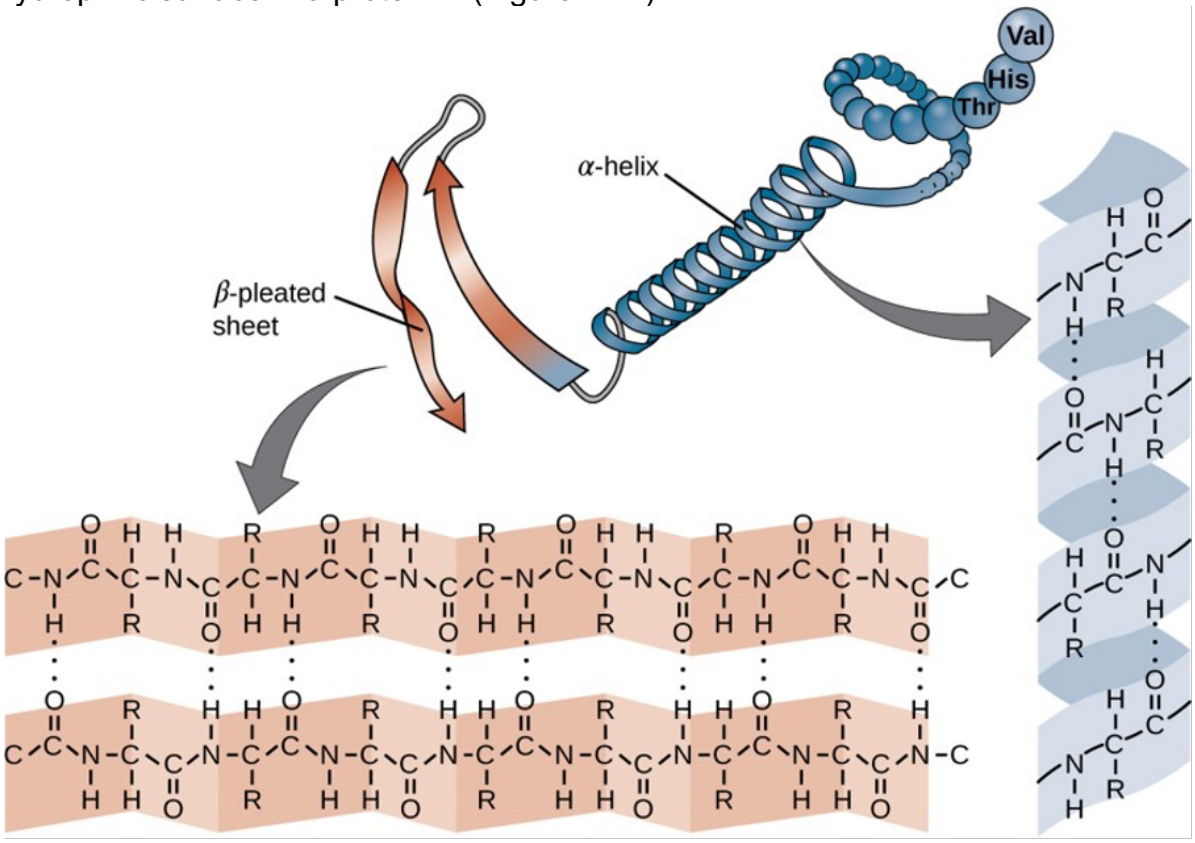

Figure 1.11 *Secondary Structural Features in Protein Structure. The right-handed alpha helix (blue) and beta-pleated sheet (orange) are common structural motifs found in most proteins. They are held together by hydrogen bonds between the amine and the carbonyl oxygen within the amino acid backbone.* [38]

1.7.3 Tertiary Structure

The tertiary structure of proteins is produced by different kinds of chemical interactions between polypeptide backbone residues, such as hydrophobic interactions (mostly between aryl/alkyl side chains), ionic interactions, hydrogen bonding and disulfide linkages (between sulfure-containing amino-acids such as Cysteine) [39] (Figure 1.12).

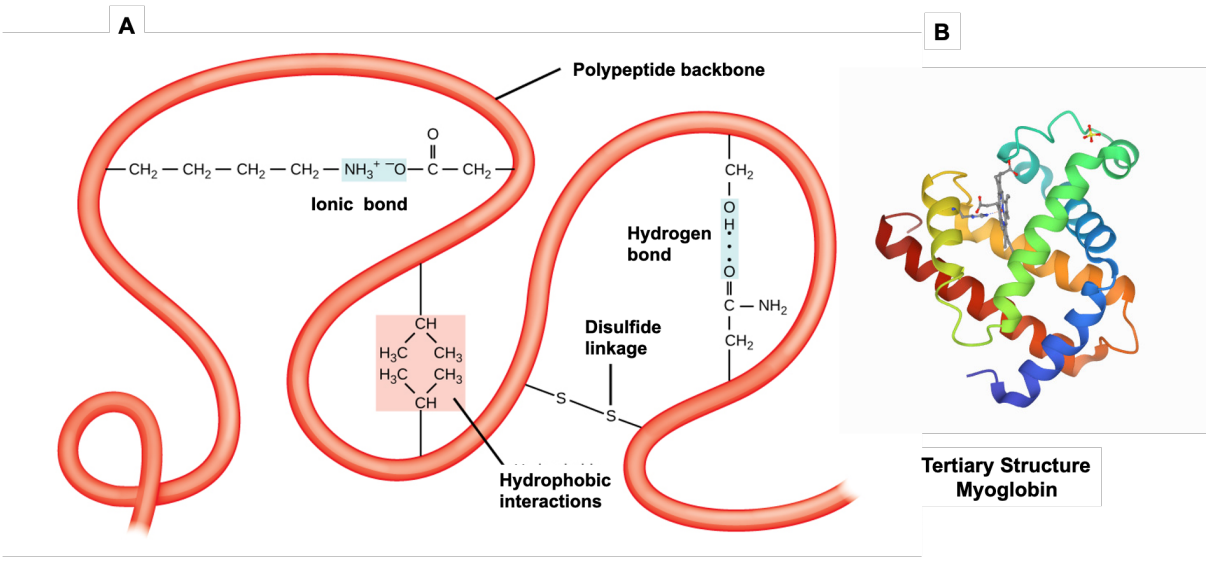

Figure 1.12 *(A) The tertiary structure of proteins forms from different kinds of chemical interactions between polypeptide backbone residues such as hydrophobic interactions, ionic interactions, hydrogen bonding and disulfide bridges [modified after [39]], (B) Tertiary structure of Myoglobin protein from Protein Data Bank (PDB:1VXA)*

1.7.4 Quaternary Structure

While many proteins consist of only a single poly-peptide chain, some consist of multi-chains. The interaction and linking of two or more motifs of tertiary protein structure gives rise to the quaternary structure. Hemoglobin is a well-known protein with a quaternary structure constituted of four myoglobin-like (tertiary structure) subunits and an heme group which contains iron. Two subunits are designated as alpha, and the two other chains are called beta (Figure 1.13 A-B). [40]

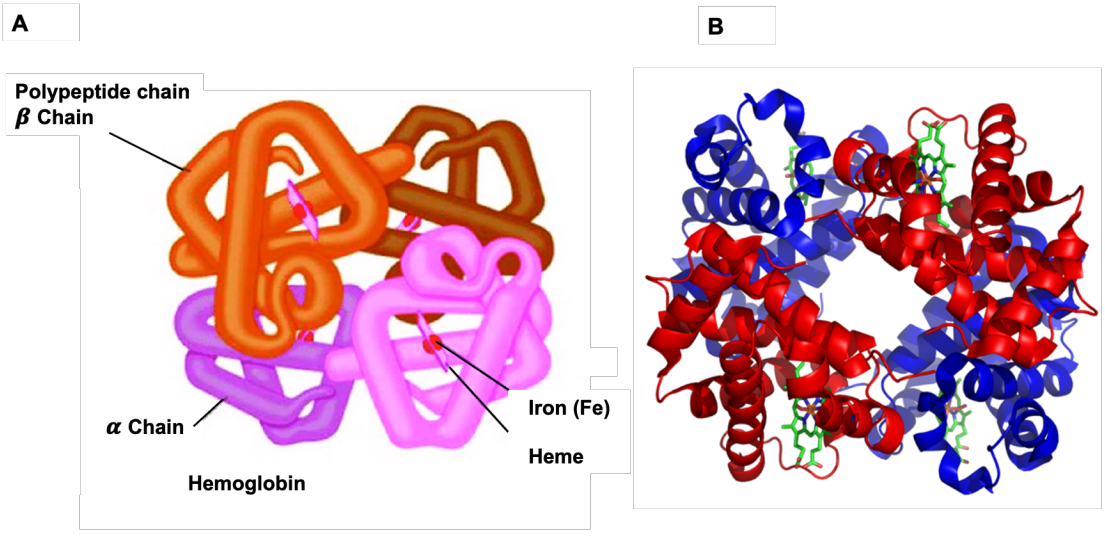

Figure 1.13 *(A) Illustration of the quaternary structure of the hemoglobin protein constituted of four subunits [after [41]] (B) Quaternary structure of human hemoglobin with α and β subunits, colored in red and blue, respectively, and four heme groups in green from PDB: 1GZX Proteopedia Hemoglobin.*

1.8 FRET in proteins

Labeling of a protein with specific fluorophores at specific sites enables measurements of structural changes of the protein in solution through FRET. In this well-known method, the protein is labeled with two fluorophores, one of them acts as an energy donor and the other one accepts the transferred energy from donor (Figure 1.14). The conformational changes within a protein have a significant effect on the distance between donor and acceptor molecules and therefore on their interaction, resulting in variations of the FRET efficiency. Because the FRET efficiency is extremely sensitive to the separation distance between donor and acceptor fluorophores, a given value of the efficiency can be assigned to a specific conformation of the protein.

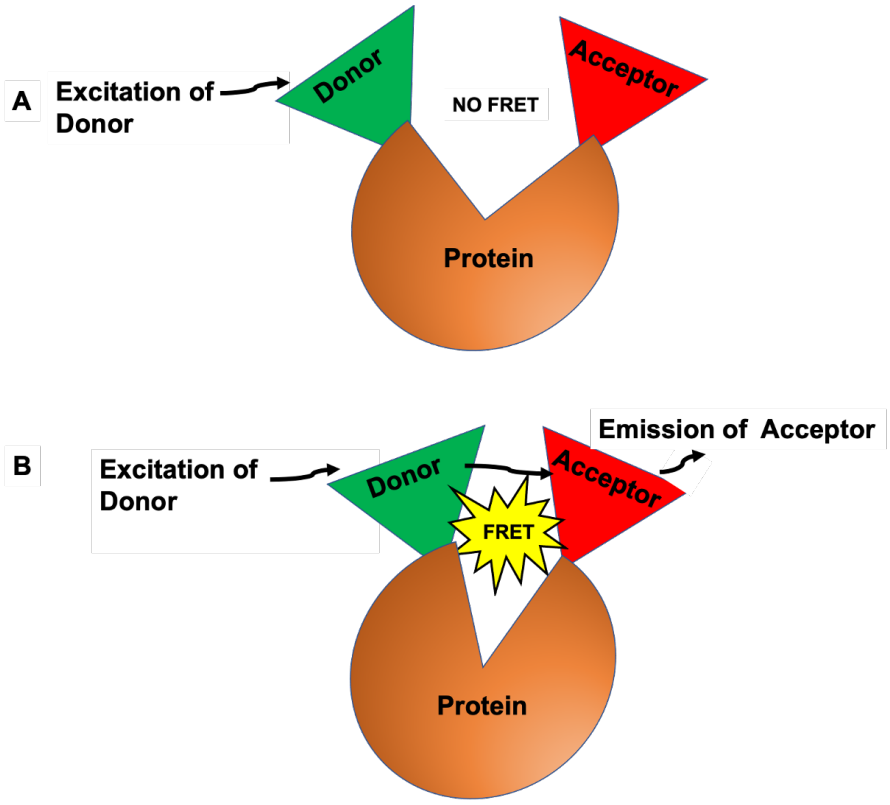

Figure 1.14 *Schematics of FRET in a doubly-labeled protein in which a donor (green) and an acceptor (red) fluorophore are attached to the same protein. The FRET interaction enables studies of conformational changes of the molecule. (A) Upon a conformational change, the distance between donor and acceptor fluorophores attached to the protein becomes r> 10 nm, thus no energy transfer takes place. (B) Upon a conformational change, the distance between donor and acceptor fluorophores attached to the protein becomes r<10 nm and, upon excitation of the donor fluorophore, FRET occurs [after* [42]*].*

The resonance energy transfer can also occur towards a non-fluorescent acceptor, for example towards a non-fluorescent absorbing metal center in a protein or towards a non-fluorescent dye attached to the protein (Figure 1.15).

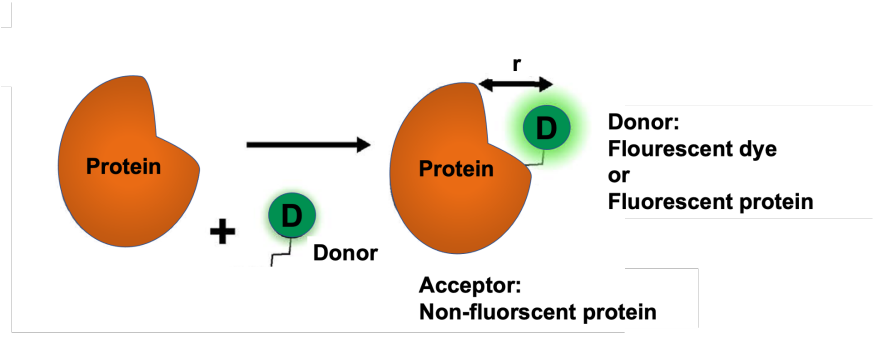

Figure 1.15 *Schematics of FRET in one labeled* ***protein*** *in which a fluorescent dye/or a fluorescent protein act as donor (green) attached to an absorbing but non-fluorescent protein as acceptor (orange). When r<10 nm, FRET occurs and fluorescent emission of donor is quenched by the absorption through the protein acceptor.*

Resonance energy transfer can thus occur between a fluorescent protein (donor) and myoglobin as nonfluorescent acceptor. For example Myoglobin-mCherry is a FRET-based probe in which the mCherry fluorescent protein (as donor) is attached to the non-fluorescent myoglobin (as acceptor) [43] [Fig. 1.16].

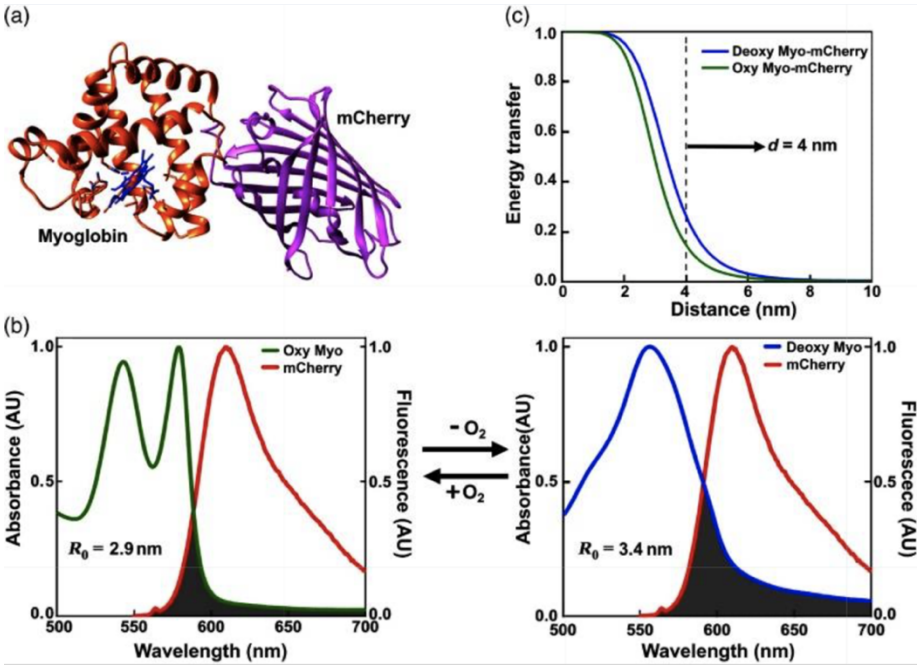

Figure 1.16 *Myoglobin-mCherry as a FRET-based probe in which the mCherry fluorescent protein (as donor, right side) is attached to the non-fluorescent myoglobin (as acceptor, left side), (B, left side) The absorption spectrum of oxymyoglobin in which myoglobin is bound to oxygen (green curve) overlaps with the emission spectrum of mCherry (red curve) and* (B, right side) *the absorption spectrum of deoxy-myoglobin in which myoglobin is unbound to oxygen (blue curve) overlaps with the emission spectrum of mCherry (red curve), Basically the spectral overlap between donor and acceptor is different when O_2 is bound (left side) and when O_2 is unbound (right side). (C) The distance between donors (oxymyoglobin/deoxy-myoglobin) and acceptor* (mCherry) *is estimated to ~4 nm by using the Protein Data Bank (PDB).* [43]

When O_2 is bound to myoglobin, forming oxymyoglobin as the acceptor, the spectral overlap of donor with the mCherry as the donor is significantly less than when O_2 is unbound to myoglobin (deoxy-myoglobin). Therefore, the mCherry's fluorescence is quenched when O_2 is unbounded and its fluorescence intensity increases significantly when O_2 is bounded to myoglobin. It should be noted that the distance between the two proteins (donor-acceptor) is defined by the linker that connects them. Thus, the FRET probe presented here is on the basis of the changes in the spectral features of the energy acceptor and not based on the distance changes between the donor and acceptor.

References

(1) Obodovskiy, I. Chapter 12 - Luminescence. In *Radiation*; Obodovskiy, I., Ed.; Elsevier, 2019; pp 207–220.

(2) Gao, R.; S. Kodaimati, M.; Yan, D. Recent Advances in Persistent Luminescence Based on Molecular Hybrid Materials. *Chem. Soc. Rev.* **2021**, *50* (9), 5564–5589.

(3) Yang, B.; Chen, G.; Ghafoor, A.; Zhang, Y.; Zhang, Y.; Zhang, Y.; Luo, Y.; Yang, J.; Sandoghdar, V.; Aizpurua, J.; Dong, Z.; Hou, J. G. Sub-Nanometre Resolution in Single-Molecule Photoluminescence Imaging. *Nat. Photonics* **2020**, *14* (11), 693–699.

(4) Sun, C.; Yang, J.; Li, L.; Wu, X.; Liu, Y.; Liu, S. Advances in the Study of Luminescence Probes for Proteins. *J. Chromatogr. B Analyt. Technol. Biomed. Life. Sci.* **2004**, *803* (2), 173–190.

(5) Srisomwat, C.; Yakoh, A.; Avihingsanon, A.; Chuaypen, N.; Tangkijvanich, P.; Vilaivan, T.; Chailapakul, O. An Alternative Label-Free DNA Sensor Based on the Alternating-Current Electroluminescent Device for Simultaneous Detection of Human Immunodeficiency Virus and Hepatitis C Co-Infection. *Biosens. Bioelectron.* **2022**, *196*, 113719.

(6) Photoluminescence. *Wikipedia*; 2022.

(7) Sinkeldam, R. W.; Greco, N. J.; Tor, Y. Fluorescent Analogs of Biomolecular Building Blocks: Design, Properties and Applications. *Chem. Rev.* **2010**, *110* (5), 2579–2619.

(8) Principles of Fluorescence Spectroscopy - Joseph R. Lakowicz - Google Boeken https://books.google.nl/books/about/Principles_of_Fluorescence_Spectroscopy.html?id=3QKTAQAACAAJ&redir_esc=y (accessed 2022 -04 -01).

(9) Omary, M. A.; Patterson, H. H. Luminescence, Theory. In *Encyclopedia of Spectroscopy and Spectrometry*; Elsevier, 2017; pp 636–653.

(10) Theory and Calculation of the Phosphorescence Phenomenon | Chemical Reviews https://pubs.acs.org/doi/10.1021/acs.chemrev.7b00060 (accessed 2022 -04 -01).

(11) Litvinenko, K. L.; Webber, N. M.; Meech, S. R. Internal Conversion in the Chromophore of the Green Fluorescent Protein: Temperature Dependence and Isoviscosity Analysis. *J. Phys. Chem. A* **2003**, *107* (15), 2616–2623.

(12) Marian, C. M. Spin–Orbit Coupling and Intersystem Crossing in Molecules. *WIREs Comput. Mol. Sci.* **2012**, *2* (2), 187–203.

(13) Gehlen, M. H. The Centenary of the Stern-Volmer Equation of Fluorescence Quenching: From the Single Line Plot to the SV Quenching Map. *J. Photochem. Photobiol. C Photochem. Rev.* **2020**, *42*, 100338.

(14) Tanwar, A. S.; Parui, R.; Garai, R.; Chanu, M. A.; Iyer, P. K. Dual "Static and Dynamic" Fluorescence Quenching Mechanisms Based Detection of TNT via a Cationic Conjugated Polymer. *ACS Meas. Sci. Au* **2022**, *2* (1), 23–30.

(15) Tinoco, I.; Gonzalez, R. L. Biological Mechanisms, One Molecule at a Time. *Genes Dev.* **2011**, *25* (12), 1205–1231.

(16) Harroun, S. G.; Lauzon, D.; Ebert, M. C. C. J. C.; Desrosiers, A.; Wang, X.; Vallée-Bélisle, A. Monitoring Protein Conformational Changes Using Fluorescent Nanoantennas. *Nat. Methods* **2022**, *19* (1), 71–80.

(17) Hwang, H.; Myong, S. Protein Induced Fluorescence Enhancement (PIFE) for Probing Protein-Nucleic Acid Interactions. *Chem. Soc. Rev.* **2014**, *43* (4), 1221–1229.

(18) Swinehart, D. F. The Beer-Lambert Law. *J. Chem. Educ.* **1962**, *39* (7), 333.

(19) Tian, Y.; Halle, J.; Wojdyr, M.; Sahoo, D.; Scheblykin, I. G. Quantitative Measurement of Fluorescence Brightness of Single Molecules. *Methods Appl. Fluoresc.* **2014**, *2* (3), 035003.

(20) Crosby, G. A.; Demas, J. N.; Callis, J. B. Absolute Quantum Efficiencies. *J. Res. Natl. Bur. Stand. Sect. Phys. Chem.* **1972**, *76A* (6), 561–577.

(21) Fluorescence Lifetime Measurements and Biological Imaging | Chemical Reviews https://pubs.acs.org/doi/10.1021/cr900343z (accessed 2022 -04 -01).

(22) Förster, Th. Zwischenmolekulare Energiewanderung und Fluoreszenz. *Ann. Phys.* **1948**, *437* (1–2), 55–75.

(23) Lee, S.; Lee, J.; Hohng, S. Single-Molecule Three-Color FRET with Both Negligible Spectral Overlap and Long Observation Time. *PloS One* **2010**, *5* (8), e12270.

(24) Lerner, E.; Barth, A.; Hendrix, J.; Ambrose, B.; Birkedal, V.; Blanchard, S. C.; Börner, R.; Sung Chung, H.; Cordes, T.; Craggs, T. D.; Deniz, A. A.; Diao, J.; Fei, J.; Gonzalez, R. L.; Gopich, I. V.; Ha, T.; Hanke, C. A.; Haran, G.; Hatzakis, N. S.; Hohng, S.; Hong, S.-C.; Hugel, T.; Ingargiola, A.; Joo, C.; Kapanidis, A. N.; Kim, H. D.; Laurence, T.; Lee, N. K.; Lee, T.-H.; Lemke, E. A.; Margeat, E.; Michaelis, J.; Michalet, X.; Myong, S.; Nettels, D.; Peulen, T.-O.; Ploetz, E.; Razvag,

Y.; Robb, N. C.; Schuler, B.; Soleimaninejad, H.; Tang, C.; Vafabakhsh, R.; Lamb, D. C.; Seidel, C. A.; Weiss, S. FRET-Based Dynamic Structural Biology: Challenges, Perspectives and an Appeal for Open-Science Practices. *eLife* **2021**, *10*, e60416.

(25) Sikor, M. Single-molecule fluorescence studies of Protein Folding and Molecular Chaperones. Text.PhDThesis, Ludwig-Maximilians-Universität München, 2011.

(26) Stryer, L. Fluorescence Energy Transfer as a Spectroscopic Ruler. *Annu. Rev. Biochem.* **1978**, *47* (1), 819–846.

(27) Ishikawa-Ankerhold, H. C.; Ankerhold, R.; Drummen, G. P. C. Advanced Fluorescence Microscopy Techniques—FRAP, FLIP, FLAP, FRET and FLIM. *Molecules* **2012**, *17* (4), 4047–4132.

(28) Sustarsic, M.; Kapanidis, A. N. Taking the Ruler to the Jungle: Single-Molecule FRET for Understanding Biomolecular Structure and Dynamics in Live Cells. *Curr. Opin. Struct. Biol.* **2015**, *34*, 52–59.

(29) Pradhan, B.; Engelhard, C.; Mulken, S. V.; Miao, X.; Canters, G. W.; Orrit, M. Single Electron Transfer Events and Dynamical Heterogeneity in the Small Protein Azurin from Pseudomonas Aeruginosa. *Chem. Sci.* **2020**, *11* (3), 763–771.

(30) Elliott, A. D. Confocal Microscopy: Principles and Modern Practices. *Curr. Protoc. Cytom.* **2020**, *92* (1), e68.

(31) Marvin, M. Microscopy Apparatus. US3013467A, December 19, 1961.

(32) Reilly, W. M.; Obara, C. J. Advances in Confocal Microscopy and Selected Applications. *Methods Mol. Biol. Clifton NJ* **2021**, *2304*, 1–35.

(33) Wahl, M. Time-Correlated Single Photon Counting. 14.

(34) Murray, J. E.; Laurieri, N.; Delgoda, R. Proteins. In *Pharmacognosy*; Elsevier, 2017; pp 477–494.

(35) Amino Acid. *Wikipedia*; 2022.

(36) Chapter 2: Protein Structure – Chemistry https://wou.edu/chemistry/courses/online-chemistry-textbooks/ch450-and-ch451-biochemistry-defining-life-at-the-molecular-level/chapter-2-protein-structure/ (accessed 2022 -04 -01).

(37) Kamtekar, S.; Schiffer, J. M.; Xiong, H.; Babik, J. M.; Hecht, M. H. Protein Design by Binary Patterning of Polar and Nonpolar Amino Acids. *Science* **1993**, *262* (5140), 1680–1685.

(38) File:Secondary.jpg - The School of Biomedical Sciences Wiki https://teaching.ncl.ac.uk/bms/wiki/index.php/File:Secondary.jpg (accessed 2022 -04 -01).

(39) Rehman, I.; Kerndt, C. C.; Botelho, S. Biochemistry, Tertiary Protein Structure. In *StatPearls*; StatPearls Publishing: Treasure Island (FL), 2022.

(40) Smith, A. M. CHAPTER 1 Interaction of Metal Ions with Proteins as a Source of Inspiration for Biomimetic Materials. **2015**, 1–31.

(41) Figure 2-Structure of hemoglobin showing its alpha and beta subunits... https://www.researchgate.net/figure/Structure-of-hemoglobin-showing-its-alpha-and-beta-subunits-and-the-heme-moiety-Source_fig1_221925240 (accessed 2022 -04 -01).

(42) Patel, M. J.; Yilmaz, G.; Bhatia, L.; Biswas-Fiss, E. E.; Biswas, S. B. Site-Specific Fluorescence Double-Labeling of Proteins and Analysis of Structural Changes in Solution by Fluorescence Resonance Energy Transfer (FRET). *MethodsX* **2018**, *5*, 419–430.

(43) Penjweini, R.; Andreoni, A.; Rosales, T.; Kim, J.; Brenner, M. D.; Sackett, D. L.; Chung, J. H.; Knutson, J. R. Intracellular Oxygen Mapping Using a Myoglobin-MCherry Probe with Fluorescence Lifetime Imaging. *J. Biomed. Opt.* **2018**, *23* (10), 1–14.